

# Interaction and motion of solitons in passively-mode-locked fiber lasers

Xueming Liu\*

*State Key Laboratory of Transient Optics and Photonics, Xi'an Institute of Optics and Precision Mechanics,  
Chinese Academy of Sciences, Xi'an 710119, China*

(Received 19 August 2011; published 14 November 2011)

Interaction and motion of multiple solitons in passively-mode-locked (PML) fiber lasers are investigated numerically. Three types of relative motions of two solitons are found in PML fiber lasers. The numerical results show that the relative motion of solitons attributes to the phase shift, which corresponds to the instantaneous frequency at pulse peak to be nonzero. Different from the classical dynamics of billiard balls, the interaction of solitons is similar to the Feynman diagram which is a pictorial way to represent the interaction of particles. After solitons interact with one another, their shapes do not change, but their phases shift and relative motions change. The theoretical results demonstrate that the separation of neighboring solitons in the laser cavity is about several hundred picoseconds to several nanoseconds. The theoretical predictions are in good agreement with the experimental results.

DOI: [10.1103/PhysRevA.84.053828](https://doi.org/10.1103/PhysRevA.84.053828)

PACS number(s): 42.65.Tg, 42.81.Dp, 42.55.Wd, 42.65.Re

## I. INTRODUCTION

Passively mode-locked (PML) fiber lasers can provide simple and economic ultrashort-pulse sources [1–4]. They constitute an ideal platform for exploring new areas of nonlinear dynamics [5]. Multiple soliton operation in PML fiber lasers, which has been investigated extensively [2–6], is the typical result of the conjunction of a relatively strong pumping power. Solitons observed in fiber lasers exhibit special features such as soliton bounding, soliton bunching, and quasiharmonic and harmonic mode locking. Bound solitary pulses, so-called soliton molecules [2,7], have attracted a great deal of interest due to their important potential applications. Bound states of solitons can be predicted in the coupled nonlinear Schrödinger equations (NLSEs) [7,8] and the quintic complex Ginzburg-Landau equation [9]. Investigations of the interaction between the bound solitons show that the bound pulses always behave as a unit. Usually, the peak-to-peak (PP) separation of bound solitons is less than several-pulse duration [2,7–9].

Different from the bound states of solitons, the PP separation of soliton bunching can be over ten times larger than the pulse width. Pulse bunching is a special behavior that corresponds to the ability of several identical soliton pulses to cluster themselves in a packet.

The formation and evolution of multiple solitons have been studied numerically and experimentally by many authors [3,8,10,11]. Various features such as the pump power hysteresis, multisoliton generation, and various modes of multisoliton operation were observed experimentally and investigated theoretically. Tang *et al.* proved that the soliton shaping of the dispersive waves or the continuous-wave (cw) components plays a key role on the generation of additional solitons [8]. In our previous reports, it is proved that the mechanism of pulse splitting determines the dual- and multisoliton generation in the net-anomalous-dispersion fiber lasers [12], whereas two pulses are gradually formed at the cost of dropping off a pulse in the net-normal-dispersion fiber lasers [7]. Theoretical and experimental results show that the PML fiber lasers alternately

evolve on the stable and unstable mode-locking states as a function of the pump strength [3].

An important characteristic of the multisoliton operation of the laser is that solitons always have erratic motions. A typical experimental result is demonstrated in Fig. 1. The experimental setup and parameters are shown in our previous paper [12]. The experimental observations show that solitons in the cavity have erratic relative motions. It is important to have a clear understanding of the physical mechanism responsible for the relative motion of solitons in the PML fiber lasers.

Although some numerical and experimental investigations for multisoliton operation were reported [3,8,13,14], the investigations for a physical mechanism describing the multisoliton behavior are scarce. In our previous paper [12], although the multisoliton formation and evolution were studied numerically and experimentally in PML fiber lasers, the physical mechanism is ignored. How many types of relative motions of intracavity solitons are there in PML fiber lasers? What is the inherent mechanism that causes the intracavity solitons to have erratic relative motions and stabilize themselves at more or less random relative positions? This paper answers these questions: Three types of relative motions of solitons are found. The numerical simulations show that solitons have exactly the same pulse properties when they are at the steady state. It is found that the phase shift determines what and how solitons move. Soliton collision in PML fiber lasers is similar to the Feynman diagram, rather than the billiard ball collision.

## II. MODELING

In this paper, the nonlinear polarization evolution technique contributes to the passive mode locking of the laser. The two coupled NLSEs that involve a vector electric field can model the light-wave propagation in the weakly birefringent fibers accurately. The coupled equations are expressed by [3,15,16]

$$\begin{aligned} \frac{\partial u}{\partial z} = & -\frac{\alpha}{2}u - \delta \frac{\partial u}{\partial T} - i \frac{\beta_2}{2} \frac{\partial^2 u}{\partial T^2} + i\gamma \left( |u|^2 + \frac{2}{3}|v|^2 \right) u \\ & + \frac{g}{2}u + \frac{g}{2\Omega_g^2} \frac{\partial^2 u}{\partial T^2}, \end{aligned}$$

\*liuxueming72@yahoo.com

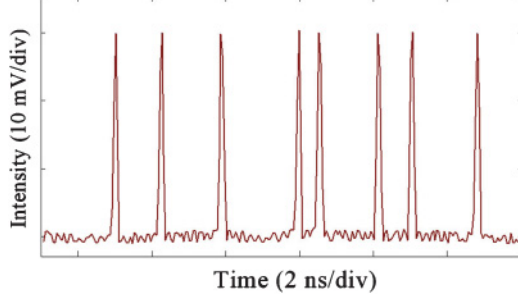


FIG. 1. (Color online) A typical example for the experimentally measured oscilloscope trace of the multisoliton operation of the PML fiber laser. The separation of neighboring solitons is about several hundred picoseconds to several nanoseconds. The output average power is  $\sim 1.2$  mW.

$$\frac{\partial v}{\partial z} = -\frac{\alpha}{2}v + \delta \frac{\partial v}{\partial T} - i \frac{\beta_2}{2} \frac{\partial^2 v}{\partial T^2} + i\gamma \left( |v|^2 + \frac{2}{3}|u|^2 \right) v + \frac{g}{2}v + \frac{g}{2\Omega_g^2} \frac{\partial^2 v}{\partial T^2}, \quad (1)$$

where  $u$  and  $v$  denote the envelopes of the optical pulses along the two orthogonal polarization axes of the fiber. They are complex functions that depend on  $T$  and  $z$ .  $T$  and  $z$  represent the time and the propagation distance, respectively.  $\alpha$ ,  $\delta$ ,  $\beta_2$ ,  $\gamma$ , and  $\Omega_g$  are the loss coefficient of the fiber, the group velocity difference between the two polarization modes, the fiber dispersion, the cubic refractive nonlinearity of the medium, and the bandwidth of the laser gain, respectively.  $g$  is the net gain, which describes the gain function of the doped fiber. It is expressed by  $g = g_0 \exp(-E_p/E_s)$  [17], where  $g_0$ ,  $E_s$ , and  $E_p$  are the small-signal gain, the gain saturation energy (it is pump-power dependent [3]), and the pulse energy, respectively. When the soliton propagates through the laser cavity, the intensity transmission  $T_i$  is expressed as

$$T_i = \sin^2(\theta) \sin^2(\varphi) + \cos^2(\theta) \cos^2(\varphi) + 0.5 \sin(2\theta) \sin(2\varphi) \cos(\phi_1 + \phi_2), \quad (2)$$

where  $\phi_1$  is the phase delay caused by the polarization controllers and  $\phi_2$  is the phase delay resulting from the fiber, including both the linear phase delay and the nonlinear phase delay. The polarizer and analyzer have an orientation of angles  $\theta$  and  $\varphi$  with respect to the fast axis of the fiber, respectively [3]. The diagram for  $\theta$  and  $\varphi$  is illustrated in Refs. [3,15] in detail.

The following parameters are employed for our simulations for possibly matching the experimental conditions:  $\alpha = 0.2$  dB/km,  $g_0 = 2$  m $^{-1}$ ,  $\theta = \pi/3.5$ ,  $\varphi = \pi/10$ ,  $\phi_1 = 0.9 + \pi/2$ ,  $\gamma = 4.5$  W $^{-1}$  km $^{-1}$  for erbium-doped fiber (EDF) and  $1.3$  W $^{-1}$  km $^{-1}$  for single-mode fiber (SMF),  $\Omega_g = 30$  nm, and  $\beta_2 = 53.5 \times 10^{-3}$  ps $^2$ /m for EDF and  $-21.7 \times 10^{-3}$  ps $^2$ /m for SMF. The lengths of EDF and SMF are 11 and 702 m, respectively. The above parameters are from the data sheets of fiber products. Obviously, the net dispersion of the laser cavity is anomalous so that the laser can deliver the conventional solitons. The schematic diagram of the experimental setup is shown in Ref. [12].

### III. SIMULATION RESULTS

#### A. Intracavity two-soliton and relative motion

To find the characteristics and behaviors of solitons in the proposed laser, the simulation starts from a noise signal and converges into a stable solution at different  $E_s$ . Since the saturation energy  $E_s$  is proportional to the pumping strength, the increase of  $E_s$  in simulations corresponds to increasing the pump power in the experiments [15]. Numerical results show that the pulse number over a cavity round-trip time is generated one by one with the increase of the pumping strength  $E_s$ . When  $E_s$  is lower than  $\sim 15$  pJ, no soliton solution exists in the proposed laser. When  $E_s$  is from  $\sim 15$  to 50 pJ, only one soliton exists in the laser cavity. However, there are two solitons simultaneously in the laser cavity while  $E_s$  is from  $\sim 50$  to 90 pJ.

Figure 2 shows the formation and evolution of two solitons from a noise signal at  $E_s = 70$  pJ. In simulations, a noise wave is assumed as an initial value. A soliton is formed first and successively split into two solitons. The detailed process is shown in Fig. 2(a). Figure 2(b), which is the planform of Fig. 2(a), shows the soliton trajectory in round-trip number  $N$  and time space. We can see from Figs. 2(a) and 2(d) that there is chaos process when a soliton is split into two solitons. From Figs. 2(a) and 2(b), one can see that the PP separation of two solitons increases in the beginning of the round trips and then it gradually approaches a fixed value of  $\sim 1.9$  ns. Numerical results show that two solitons have exactly the same physics properties (e.g., the same pulse duration and peak power) throughout the evolution of solitons. It is found from Fig. 2(d) that the peak power and pulse duration are oscillating at  $N < 120$  and successively they approach  $\sim 20.9$  W and 3.4 ps, respectively. In the steady state, the PP separation of solitons is  $\sim 560$  times as large as the pulse duration.

Figures 2(c) shows the relationship between the instantaneous frequency of the soliton at pulse peak,  $F_P$ , and round-trip number  $N$ . We can observe that, for  $N < 11$ , there is only one soliton [Fig. 2(b)] and  $F_P$  is equal to zero. Successively, a soliton is split into two solitons. When  $N$  is from  $\sim 13$  to 400, two solitons separate from each other gradually [Figs. 2(a) and 2(b)] whereas  $F_P$  gradually approaches zero [Fig. 2(c)]. For  $N > 600$ , two solitons reach the steady state with a fixed separation of  $\sim 1.9$  ns and  $F_P$  is approximately equal to zero.

When  $E_s$  is from  $\sim 75$  to 82 pJ, the relative motion of the two solitons is different from Fig. 2 where each soliton approaches a certain position. An example for the evolution of two solitons at  $E_s = 81$  pJ is shown in Fig. 3. One can see from Fig. 3(a) that one of the solitons evolves to a fixed position whereas the other soliton oscillates with an amplitude of  $\sim 100$  ps and a period of 118 round trips. The PP separation of the two solitons periodically oscillates from  $\sim 360$  to 460 ps for  $N > 400$ . It is found that  $F_P$  of the oscillating soliton also periodically oscillates along  $N$  [Fig. 3(b)], while  $F_P \approx 0$  for the fixed soliton.

When  $E_s$  is from  $\sim 82$  to 90 pJ, both  $F_P$  and two solitons oscillate along  $N$ . Figure 4 demonstrates the evolution of two solitons at  $E_s = 85$  pJ. Figure 4(a) shows that two solitons oscillate with an amplitude of  $\sim 117$  ps and the period of 119 round trips. Two solitons attract and repel each other

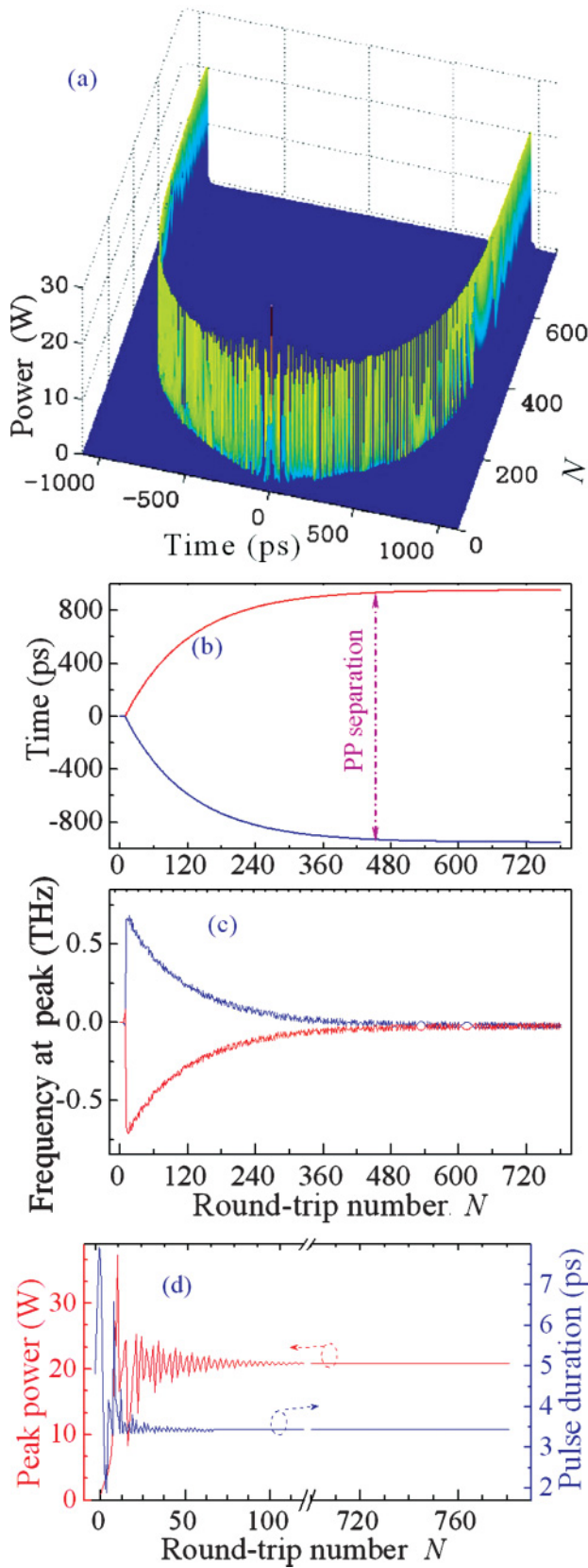


FIG. 2. (Color online) (a) Formation and evolution of solitons from a noise wave. (b) Soliton trajectory in round-trip number  $N$  and time space. (c) Instantaneous frequency at pulse peak,  $F_p$ , versus  $N$ . (d) Peak power and pulse duration versus  $N$ . (b) is the planform of (a).  $E_s = 70$  pJ.

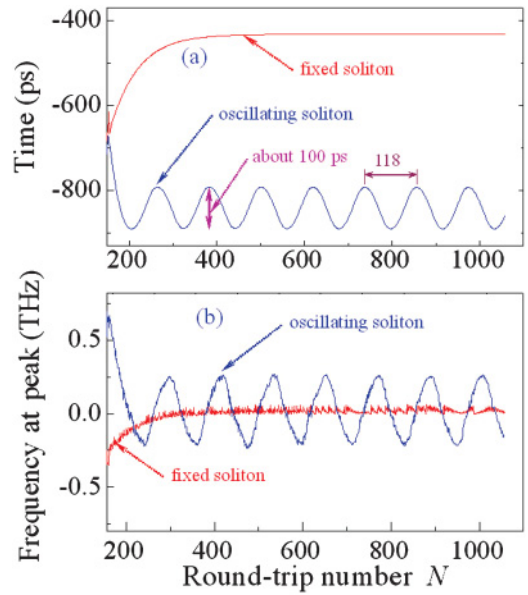


FIG. 3. (Color online) Evolution of two solitons at  $E_s = 81$  pJ. (a) Soliton trajectory in round-trip number  $N$  and time space. (b) Instantaneous frequency at pulse peak,  $F_p$ , versus  $N$ .

periodically along  $N$ . The PP separation of solitons periodically oscillates from  $\sim 415$  to  $690$  ps for  $N > 150$  [Fig. 4(a)].

Obviously, there are three types of relative motions for two solitons in the laser cavity. They evolve with the fixed trajectory (Fig. 2) and the oscillating trajectory for both of two solitons (Fig. 4), as well as the fixed trajectory for one soliton and the oscillating trajectory for another soliton (Fig. 3). The instantaneous frequency at pulse peak,  $F_p$ , governs the relative motion of solitons. Solitons evolve to the steady state when  $F_p$  approaches zero, whereas they oscillate in the cavity for  $F_p \neq 0$ . For example, as shown in Fig. 2, two solitons

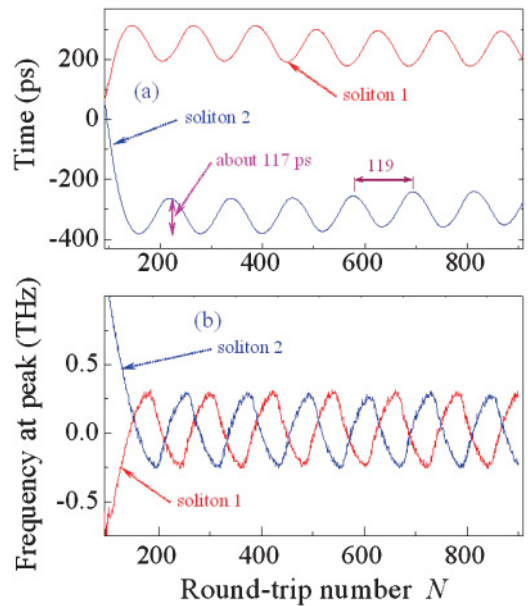


FIG. 4. (Color online) Evolution of two solitons at  $E_s = 85$  pJ. (a) Soliton trajectory in round-trip number  $N$  and time space. (b) Instantaneous frequency at pulse peak,  $F_p$ , versus  $N$ .

have the same pulse properties (e.g., the same pulse duration, pulse energy, and phase) with a fixed separation. In this case, the unit of two solitons is very similar to the bound-state solitons except that they have different PP separations. This type of soliton pair can be regarded as a static soliton pair. When the relative motion of one or two solitons is oscillating (e.g., Figs. 3 and 4), this kind of soliton pair can be regarded as a dynamic soliton pair. The theoretical results explain why the intracavity multisolitons can have erratic relative motions in the experimental observations.

### B. Intracavity multisoliton and collision

When  $E_s$  is from  $\sim 90$  to 125 pJ, three solitons with the same physical properties coexist in the cavity. An example for  $E_s = 96.2$  pJ is shown in Fig. 5. One can see that, for  $N > 900$ ,  $F_P$  per soliton is approximately equal to zero [Fig. 5(c)] and each soliton evolves to the steady state [Fig. 5(a)]. The three solitons have the same pulse profile, pulse duration, and peak power. From Figs. 5(a) and 5(b), we can find a strange phenomenon when  $N$  is from  $\sim 475$  to 500. At this stage, two solitons repel each other and never merge. The inset of Fig. 5(b) shows that the minimum separation of neighboring solitons is  $\sim 35$  ps.

According to soliton theory, when solitons interact with other solitons, their shapes do not change, but their phase shifts. Actually, the phenomenon of “phase shift” is a standard feature of soliton interactions. The change of phase leads to the variation of  $F_P$ . Note that the instantaneous frequency is the first derivative of phase [18]. Obviously, the numerical simulations here are in excellent agreement with the results in the traditional soliton theory. The theoretical prediction in this paper is very similar to the Korteweg-de Vries (KdV) soliton in Ref. [19]. Moreover, Fig. 5(c) shows that  $F_P$  at the soliton collision ( $N \approx 475$ –500) has a strong fluctuation and a strong phase shift occurs.

When  $E_s$  is from  $\sim 125$  to 155, 155 to 185, and 185 to 205 pJ, numerical results shows that four, five, and six solitons coexist in the laser cavity, respectively. Figures 6(a), 6(b), and 6(c) demonstrate three examples at  $E_s = 130$ , 165, and 200 pJ, respectively. In the simulation, the phase shifts are imposed on some solitons initially. The simulation results exhibit that the solitons imposed by the initial phase shift have relative motion in the beginning of round trips. After enough round trips, all solitons approach the steady state and  $F_P$  of each soliton is near zero. In simulating Fig. 6(c), only one soliton is initially imposed on the phase shift, but the soliton collisions occur four times. Figures 5 and 6 illustrate that the separation of neighboring solitons is nonuniform and the numerical predictions agree well with the experimental observations as shown in Fig. 1. From Figs. 2–6, one can see that the PP separation of neighboring solitons is about several hundred picoseconds to several nanoseconds. The experimental results (e.g., Fig. 1) confirm the theoretical predictions.

We can see from Figs. 5 and 6 that, as two solitons get close, they never pass through each other and the transfers of energy and information of solitons are transited by a virtual soliton. Obviously, Figs. 5 and 6 show that the soliton collision in PML fiber lasers is not similar to the billiard ball collision. Rather than the classical dynamics of billiard balls, the interaction of solitons can similarly be interpreted by the Feynman diagram,

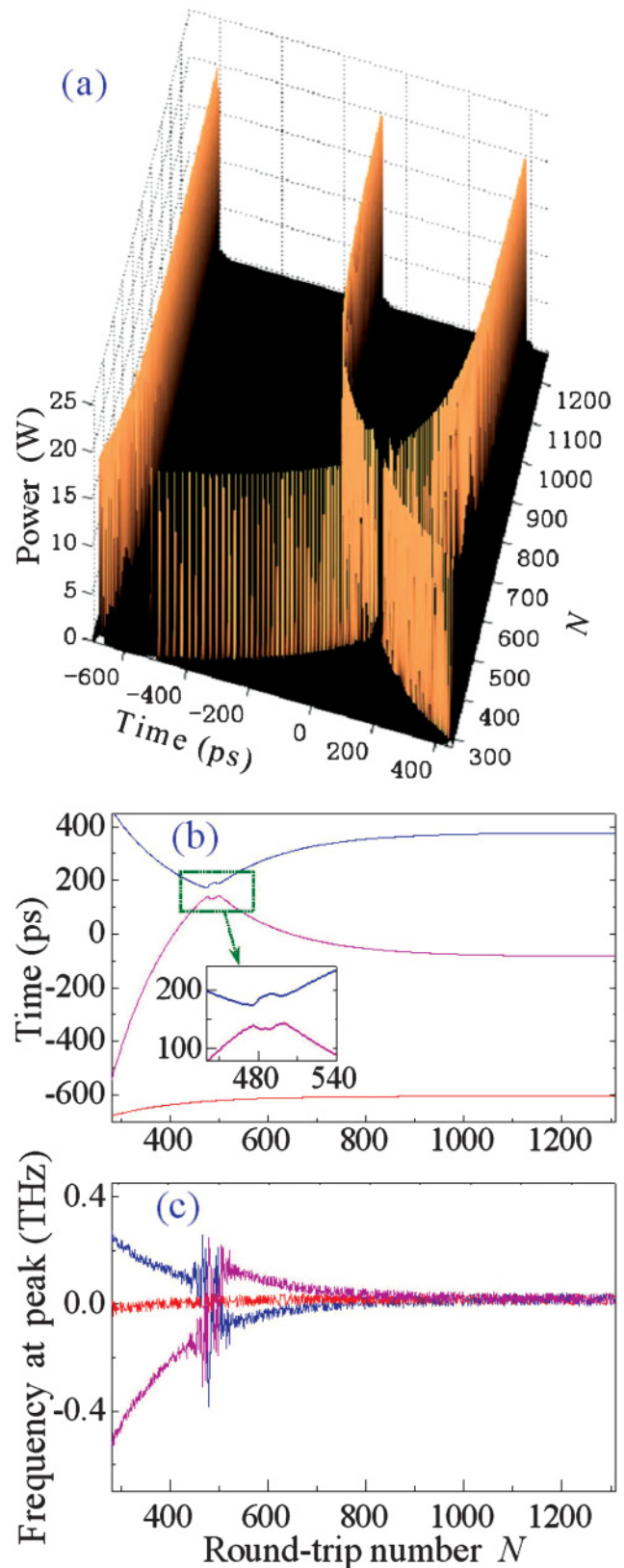


FIG. 5. (Color online) (a) Interaction and evolution of three solitons at  $E_s = 96.2$  pJ. (b) Soliton trajectory in round-trip number  $N$  and time space. (c) Instantaneous frequency at pulse peak,  $F_P$ , versus  $N$ . In (b), inset is the local view of the soliton collision. In (c),  $F_P$  at  $N \approx 475$ –500 has a strong fluctuation and a strong phase shift is incurred.

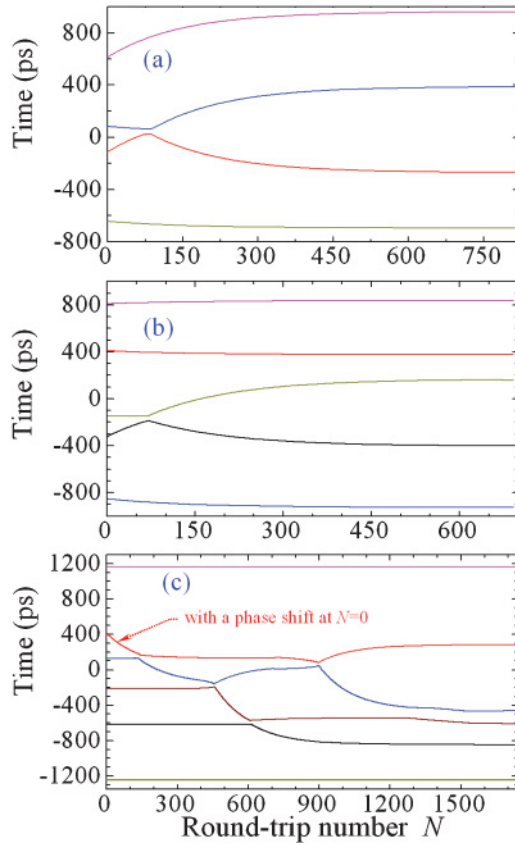


FIG. 6. (Color online) Soliton trajectory in round-trip number  $N$  and time space at (a)  $E_s = 130$  pJ, (b)  $E_s = 165$  pJ, and (c)  $E_s = 200$  pJ. Four, five, and six solitons coexist in the laser cavity for (a), (b), and (c), respectively. Although some neighboring solitons get close and collide, they never pass through each other. In (c), only a soliton is initially imposed on a phase shift, but the soliton collisions occur four times.

in which during their interaction, two electrons exchange a (virtual) photon and then repel one other [20]. In fact, the particlelike behavior of solitons is discovered in the KdV two-soliton collision, where a virtual “transfer” soliton steals energy from the faster one in the rear and passes it to the soliton in front [19,21]. As a result, solitons are waves that act like particles and even the particlelike behavior of solitons can help us to better understand real particles.

#### IV. MECHANISM OF MOTION OF SOLITONS

When the separation of solitons is over tens times larger than the pulse duration, the interaction between solitons is very weak. What is the key role that governs the motion of solitons? From Figs. 2–6, the relative motion of solitons originates from the phase shift.

Our laser is mode locked using the nonlinear phase rotation (NPR) technique. The laser cavity can be simplified to a setup as shown in Fig. 7 [3,8]. The intensity transmission  $T_i$  from input to output, as shown in Fig. 7, can be achieved by numerically solving Eqs. (1) and (2). When no phase shift is imposed on solitons (corresponding to  $F_P = 0$ ), the intensity transmission  $T_i$  is symmetrical with respect to the relative time [Fig. 8(a)]. As a result, no relative motion occurs except that



FIG. 7. (Color online) An equivalent setup to NPR element for determining the cavity transmission.

the soliton intensity is attenuated [Fig. 8(b)]. However, when the phase shift is imposed on the soliton (corresponding to  $F_P \neq 0$ ),  $T_i$  is asymmetrical with respect to the relative time [dashed curve in Fig. 8(a)] and then the soliton has the relative motion shown as the dashed curve in Fig. 8(b).

Figure 9 shows the soliton trajectory in the intracavity position and time space. In simulations, the phase shift is imposed on soliton 1, but not on soliton 2. It is easily found from Fig. 9 that there is no relative motion for a soliton without the phase shift, whereas another soliton with the phase shift has the relative motion along the intracavity position. In our previous paper, the chirped solitons are narrowed in the beginning of the propagation distance and successively they are broadened due to the dispersive effect (Figs. 8 and 9 in Ref. [12]). But, no relative motion occurs for them, similar to soliton 2 in Fig. 9. Besides the dispersion-induced narrowing and broadening of pulses, the relative motion occurs for the solitons imposed by the phase shift (soliton 1 in Fig. 9 shows an example). Therefore, the dispersion-induced phase shift plays a key role in the relative motion of solitons in the laser cavity.

In practice, many parameters of lasers are fluctuant, such as pump power, environmental temperature, refractive index of fiber, and polarization state. These fluctuations will perturb

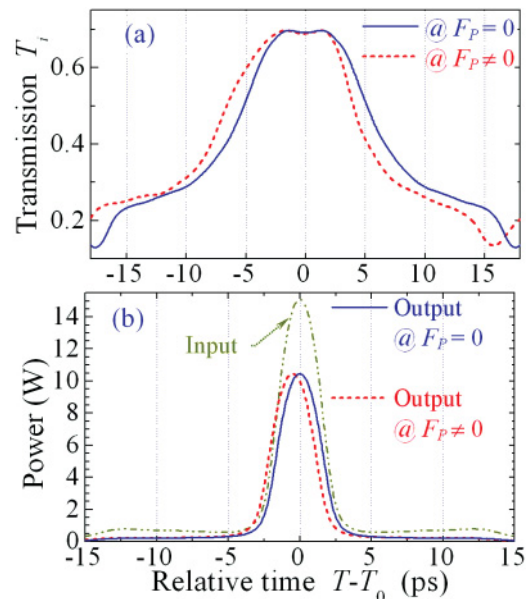


FIG. 8. (Color online) (a) Intensity transmission at  $F_P = 0$  and  $F_P \neq 0$ . (b) Power spectra of solitons before and after NPR element. The solid curve in (a) is symmetrical with respect to the relative time, but the dashed curve is asymmetrical.

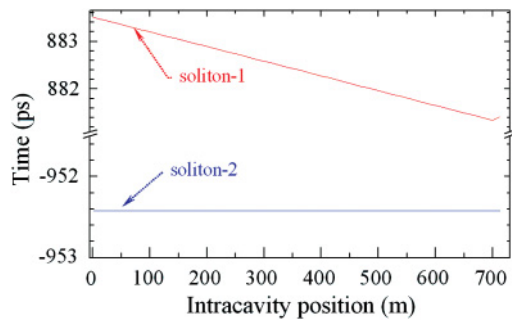


FIG. 9. (Color online) Soliton trajectory in intracavity position and time space. The phase shift is imposed on soliton 1, but not on soliton 2. There is and is not the relative motion for soliton 1 and soliton 2 along the intracavity position, respectively.

the laser system and may contribute to the phase shift of the solitons. Additionally, the soliton collision can induce a strong phase shift, as shown in Fig. 5(c). Figure 6(c) shows that the soliton collision induces the relative motions of multiple solitons along  $N$ . Therefore, intracavity solitons are easily imposed by the phase shift in a practical environment so that they often have erratic relative motions and stabilize themselves at more or less random relative positions. The theoretical results are consistent with the experimental observations.

## V. CONCLUSIONS

In this paper, we have numerically investigated the evolution and interaction of two and multiple solitons and their relative motions in PML fiber lasers with the net anomalous dispersion. Three types of relative motions of solitons are found by solving the coupled complex NLSEs. When the pumping strength  $E_s$  is lower (e.g.,  $E_s = 70$  pJ), two solitons always have exactly the same physics properties throughout

their evolution and their separation approaches a fixed value (e.g., 1.9 ns). In this case, two solitons behave as a unit and are regarded as a static soliton pair. Contrarily, one of two solitons or both oscillate with approximately fixed amplitude of relative motions and a periodic round-trip number by appropriately enhancing  $E_s$  (e.g.,  $E_s = 81$  or 85 pJ). Two solitons periodically attract and repel each other with respect to the round-trip number  $N$ . In this case, two solitons are regarded as a dynamic soliton pair. The PP separation of static and dynamic soliton pairs is over two orders of magnitude larger than the pulse duration (Figs. 2–4).

The numerical simulations show that the relative motion of solitons attributes to the phase shift, which corresponds to the instantaneous frequency at pulse peak to be nonzero. When two solitons collide, they never pass through each other and the transfers of energy and information of solitons are transited by a virtual soliton. After the collision between two solitons, their shapes do not change, but their phases shift and relative motions change. The theoretical results demonstrate that the separation of neighboring solitons in laser cavity is about several hundred picoseconds to several nanoseconds. The theoretical predictions are in good agreement with the experimental results. Our theoretical results successfully interpret why the intracavity solitons have erratic relative motions and stabilize themselves at more or less random relative positions. In addition, the particlelike behavior of solitons can help us to better understand real particles.

## ACKNOWLEDGMENTS

This work was supported by the National Natural Science Foundation of China under Grants No. 10874239 and No. 10604066. The author would especially like to thank Xiaohui Li, Dong Mao, and Lina Duan for help with the experiments.

- 
- [1] H. Zhang, Q. Bao, D. Tang, L. Zhao, and K. Loh, *Appl. Phys. Lett.* **95**, 141103 (2009); D. Mao, X. M. Liu, L. R. Wang, X. H. Hu, and H. Lu, *Laser Phys. Lett.* **8**, 134 (2011).
  - [2] M. Stratmann, T. Pagel, and F. Mitschke, *Phys. Rev. Lett.* **95**, 143902 (2005).
  - [3] X. M. Liu, *Phys. Rev. A* **81**, 023811 (2010); X. M. Liu, L. R. Wang, X. H. Li, H. B. Sun, A. X. Lin, K. Q. Lu, Y. S. Wang, and W. Zhao, *Opt. Express* **17**, 8506 (2009).
  - [4] Z. P. Sun, D. Popa, T. Hasan, F. Torrisi, F. Wang, E. J. R. Kelleher, J. C. Travers, V. Nicolosi, and A. C. Ferrari, *Nano Res.* **3**, 653 (2010).
  - [5] S. Chouli and P. Grelu, *Phys. Rev. A* **81**, 063829 (2010).
  - [6] K. Tamura, H. A. Haus, and E. P. Ippen, *Electron. Lett.* **28**, 2226 (1992).
  - [7] X. M. Liu, *Phys. Rev. A* **82**, 063834 (2010).
  - [8] D. Y. Tang, L. M. Zhao, B. Zhao, and A. Q. Liu, *Phys. Rev. A* **72**, 043816 (2005).
  - [9] A. Komarov, H. Leblond, and F. Sanchez, *Phys. Rev. E* **72**, 025604 (2005).
  - [10] A. Komarov, H. Leblond, and F. Sanchez, *Phys. Rev. A* **71**, 053809 (2005).
  - [11] F. Amrani, M. Salhi, P. Grelu, H. Leblond, and F. Sanchez, *Opt. Lett.* **36**, 1545 (2011).
  - [12] X. M. Liu, *Phys. Rev. A* **84**, 023835 (2011).
  - [13] E. D. Farnum, B. G. Bale, and J. N. Kutz, *Phys. Rev. A* **81**, 033851 (2010).
  - [14] R. Weill, B. Vodonos, A. Gordon, O. Gat, and B. Fischer, *Phys. Rev. E* **76**, 031112 (2007).
  - [15] X. M. Liu, *Phys. Rev. A* **81**, 053819 (2010); **82**, 053808 (2010).
  - [16] X. M. Liu, *Opt. Express* **19**, 5874 (2011).
  - [17] G. Agrawal, *IEEE Photonics Technol. Lett.* **2**, 875 (1990).
  - [18] G. P. Agrawal, *Nonlinear Fiber Optics*, 4th ed. (Academic Press, Boston, 2007).
  - [19] N. Benes, A. Kasman, and K. Young, *J. Nonlinear Sci.* **16**, 179 (2006).
  - [20] L. Motta, entry on Feynman Diagrams, [<http://scienceworld.wolfram.com/physics/FeynmanDiagram.html>].
  - [21] [<http://kasmana.people.cofc.edu/SOLITONPICS/>].